Electronic Supplementary Information

Title

Toward Hyperuniform Disordered Plasmonic Nanostructures for

Reproducible Surface-Enhanced Raman Spectroscopy

Claudio De Rosa, Finizia Auriemma, Claudia Diletto, Rocco Di Girolamo, Anna Malafronte.
Dipartimento di Scienze Chimiche, Università di Napoli "Federico II", Complesso Monte Sant'Angelo, Via Cintia, I-80126 Napoli, Italy

Pasquale Morvillo
ENEA Italian National Agency for New Technologies, Energy and Sustainable Development, UTTP-NANO, Piazzale E. Fermi 1, 80055 Portici, Italy

Gianluigi Zito,* Giulia Rusciano, Giuseppe Pesce, Antonio Sasso
Dipartimento di Fisica, Università di Napoli "Federico II", Complesso Monte Sant'Angelo, Via Cintia, I-80126 Napoli, Italy.

*Corresponding Author E-mail: zito@fisica.unina.it

1. Average size of gold nanoparticles

Gold nanoparticles have been produced by vacuum evaporation of gold and successive deposition onto the film surface of the phase separated BCP. The average size of the so produced Au-NPs has been evaluated from the bright-field TEM images of the nanocomposite BCP thin films. The size distribution of Au-NPs shown in Figure S1 was evaluated From the TEM images of Figures 1b,c and 2d of PS-*b*-PMMA thin films decorated with Au-NPs. The average diameter of Au-NPs was established equal to 3.9±0.9 nm.
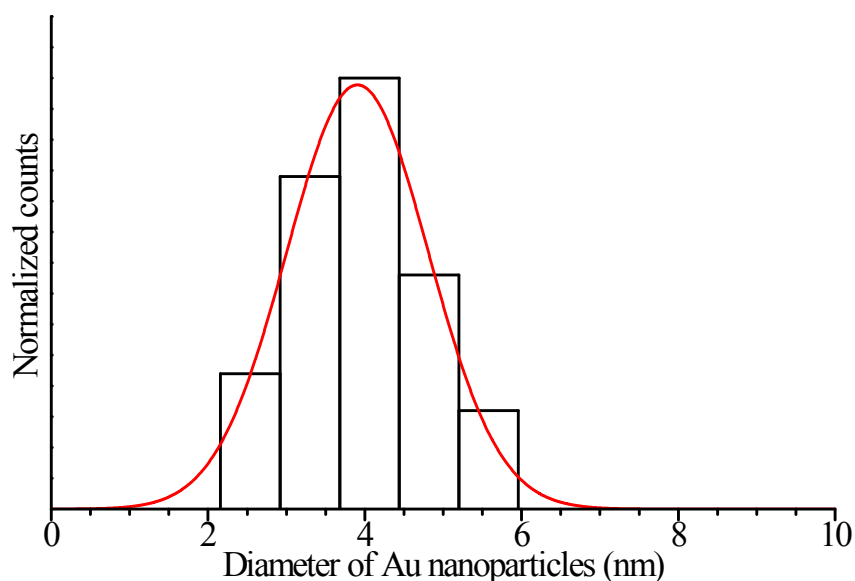
Figure S1. Typical size distribution of Au-NPs obtained by measuring the diameter of at least 100 nanoparticles in each TEM micrographs of Figures 1b, 1c and 2d.

2. Confocal micro-Raman setup

A schematic representation of the confocal micro-Raman setup used in this work, namely a *Witec Alpha 300,* is depicted in Figure S2. The micro-Raman system is endowed with a spectrometer equipped with two diffraction gratings (600 and 1800 g/mm). Backscattering collection and detection were, respectively, through a 60× dry objective and a CCD camera (1024 pixels) operating at -60 °C. In this setup, the confocal condition is imposed by the core (acting as a pin-hole) of the fiber delivering the signal to the spectrometer. The probed scattering area on the sample, constrained by confocal detection in backscattering collection, was accurately measured independently to be $\pi w_o^2 = 0.44$ μm^2 ($w_o = 373$ nm) with a knife-edge technique as described below (see section 6). A three-axis piezo-nanopositioner allowed precise control of the sampling translation and positioning on the copolymer/metal nanocomposites with nanometer accuracy over a maximum range of 100 × 100 μm^2. For larger areas, a coarse translation was added by using the mechanical micrometer of the microscope stage. This permitted to sample multiple areas of 100× 100 μm^2 within a large window of centimeter scale. Positioning, area mapping and acquisition were controlled via computer.
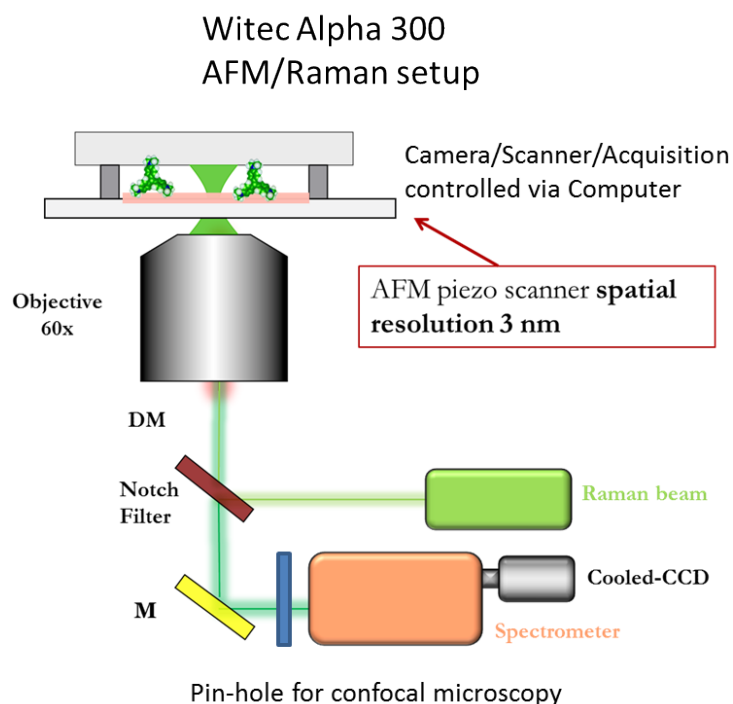
Witec Alpha 300
AFM/Raman setup

Figure S2. Schematic representation of confocal micro-Raman setup.

3. Assignment of Raman bands

Most representative peaks for PS are at 1000 cm^{-1} (C-C ring breathing mode), 1600 cm^{-1} (tangential ring stretching mode), 2904 cm^{-1} (C-H asymmetric stretching), 3054 cm^{-1} (C-H symmetric stretching). For PMMA are at 812 cm^{-1} (C-O-C symmetric stretch), 1445 cm^{-1} (CH$_2$ symmetric bend vibration), 1734 cm^{-1} (C=O stretching mode), 2930 cm^{-1} (C-H symmetric stretching) (see also refs. S1 and S2). In Table S1, assignment of Raman bands of Crystal Violet are also reported S3.

Table S1. Raman bands of Crystal Violet typically measured in SERS and single molecule (SM-SERS) (from ref. S3). ν: stretching (s: symmetric; as: antisymmetric); δ: bending; ρ: rocking; γ: out-of-plane deformation; τ: torsion.

Description of vibrations contributing to the normal modes in Crystal Violet	SERS (cm^{-1})	SM-SERS (cm^{-1})
ν_s(C-C)	1620	1622
	1587	1584
ν(C$_{ring}$N)/δ_s(CH$_3$)	1535	
δ_{as}(CH$_3$)	1474	
δ_{as}(CH$_3$)	1448	
δ(CH)/δ_s(CH$_3$)/δ(CCC)$_{ring}$	1391	
ν_{as}(CC$_{center}$C)/δ(CCC)$_{ring}$/δ(CH)	1377	
δ(CCC)$_{ring}$/ν_{as}(CC$_{center}$C)/δ(CH)	1336	
ν_{as}(CC$_{center}$C)/δ(CCC)$_{ring}$/δ(CH)	1298	
ν_{as}(CC$_{center}$C)/δ(CCC)$_{breathing}$/δ(CH)	1220	
ν_{as}(CC$_{center}$C)	1175	1176
δ(CC$_{center}$C)/ν(CN)	1123	
δ(CCC)	996	
ρ(CH$_3$) /ν(CN)	941	
δ(CC$_{center}$C)	916	914
	826	
	806	804
ν_s(CC$_{center}$C)/ν(CN)	761	
ν(CN)	726	
	623	
δ(CCC)/δ(CNC)/ν_s(CC$_{center}$C)	607	
γ(CCC)/δ(CNC)/δ(CC$_{center}$C)	561	
δ(CNC)	526	
δ(CNC)	442	
δ(CNC)/δ(CC$_{center}$C)	425	
γ(CNC)/ρ(CH$_3$)	339	
τ(CH$_3$)	209	

4. Method for uniform distribution of Crystal Violet molecules on the SERS substrates.

Tris(4-(dimethylamino)phenyl)methylium chloride (Crystal Violet, from Sigma Aldrich) was diluted into a milli-Q water solution to different concentrations, namely 3.1, 9.2, 25.3, 34.6, 43.9, 69.2, 138, 150, 380, 760, 1140, 1520 nM. Then, the employed solution was infiltrated into a cell constituted by two parallel substrates (24×24 mm^2), both B or D, distanced by silica beads spacers of variable diameter depending on the desired thickness of the cell, from 4.8 μm ($\pm$ 4%) to 15.0 μm ($\pm$ 4%). For larger thicknesses, PET spacers (Mylar) were also employed. The planar cell was sealed at two of the external borders with UV glue. With this approach, the liquid is infiltrated into a precisely controlled volume (see Figure S3). The entrance and flow windows retain the liquid to leak out by the surface tension of water (another solvent requires a different procedure). Under this condition, the water evaporates towards the center of the cell. No inhomogeneity effect (coffee-ring) is visible at an optical microscopy inspection when high concentrated solutions are infiltrated ($\approx$ 5 mM). In other words, the evaporation leaves a nearly perfect uniform layer of molecules.

Coffee-ring effect probably is still happening but, in this case, at the borders of the evaporating water surface, which is represented by the water meniscus along vertical sections of the planar cell. The water meniscus then move towards the center of the cell as the liquid evaporates and leaves adsorbed molecules on the top and bottom surfaces. The lateral surface of the parallelepiped is negligible because of the small thickness ($\approx$ 10 - 200 μm) of the cell with respect to the width ($\approx$ 24 mm). Being top and bottom substrates identical, an equal deposition of the molecules is envisaged on the two surfaces. Hence, the spatial density of molecules on each substrate can be straightforwardly estimated. The uniformity of the molecular distribution can be verified *a posteriori* by uniformity of the SERS enhancement factor as actually demonstrated for very low concentrated solution (nanomolar range) in the main paper.

As for instance, a volume of 100 μl of 380 nM solution of CV distributed over an area of 24×24 mm^2 = 576 mm^2 from a cell of thickness $t = 174$ μm produces a monolayer of molecules of number $N_{surf} = 8536 \approx 8.5 \times 10^3$ within the scattering area of 0.44 μm^2 on each of the two surfaces.

Given the effective diameter $D_{CV} \approx 1$ nm of the CV molecule (see Figure S3) covering an approximate area of 0.785 nm², and the number of molecules N_{surf} estimated in the scattering area, the filling fraction of the probed area is only ≈ 1.53 %. Thereby, the monolayer condition is well satisfied. The enhancement factors of substrate B and D were estimated under identical condition of molecular deposition just as described, with $N_{surf} = 8536 \approx 8.5 \times 10^3$. The threshold lower limit of CV molecules experimentally detectable in these experiments was of ~ 700 molecules in the scattering area, with a capability of a quantitative discrimination with differential sensitivity of ~ 60 molecules.
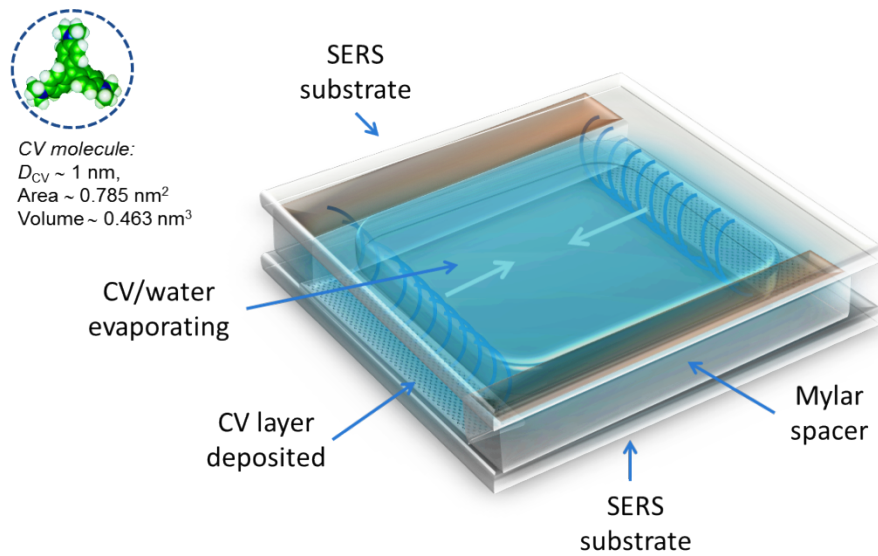

Figure S3. A cartoon representing the monolayer of CV molecules deposited onto the inner surfaces of the sandwiched SERS substrates distanced by suitable spacers.

Raman enhancements were evaluated by using the definition of the SERS *substrate enhancement factor* (*EF*) of ref. S4 , namely as

$$EF = \frac{I_{SERS} / N_{surf}}{I_{Raman} / N_{vol}},$$

where I_{SERS} and I_{Raman} are the enhanced and normal amplitudes of one Raman peak, respectively, and N_{surf} and N_{vol} are the numbers of molecules estimated in scattering area and volume, respectively. In particular, we have estimated the *EF* of our substrates by averaging the values I_{SERS}

/ I_{Raman} of six main bands of the CV, namely at 808, 914, 1175, 1370, 1585 and 1620 cm^{-1}. The scattering area collected with our setup in confocal backscattering configuration was measured by a knife-edge-like technique on a uniform SERS substrate of calibration having a sharp edge truncation on which the same collected Raman intensity was used as probe signal. The deposition was in this case realized from 100 µl of 100 nM water solution of CV uniformly distributed over the substrate of 24 × 24 mm^2. The truncation profile achieved by means of stripping part of the nanocomposite was inspected with both optical and atomic force microscope (AFM). The technique of knife-edge was employed under the assumption that only the fraction of molecules on the active surface gives rise to any detectable intensity, as experimentally verified. The measurement was repeated on a silicon wafer with a sharp edge following Cai at al. S6 obtaining the same results. Three-dimensional (3D) nano-positioning of the sample thanks to a piezo-scanner with an in-plane resolution of 3 nm and out-plane resolution of 0.2 nm allowed the 3D characterization of the scattering volume by measuring the waist as a function of the axial coordinate with 20 scansion planes above and below the minimum waist plane. The best fit of the Gaussian beam waist profiling gave a collection area equal to A_{scat} = 0.44 µm^2 with w_o = 373 nm (radius of waist) in agreement with the value expected for our microscope configuration. Similarly to Rayleigh length estimation for the depth of field of Gaussian beams, we estimated a 'Raman' depth of d_R = 1.5 µm. We then measured the scattering volume thickness on silicon wafer following Cai *et al*. S6 determining an effective thickness of h = 2.6 µm, in good agreement with the former value ($h = 2 \, d_R$). Therefore, the total scattering volume was determined to be V_{scat} = 2.0 µm^3, obtained from the numerical integration of a Gaussian beam volume of thickness h and waist w_o = 373 nm.

Hence, for the *EF* evaluation, the Raman reference signal I_{RS} of CV was estimated following the procedure described in ref. S5 by measuring the average scattering from a layer of CV powder, and estimating the related number of molecules in scattering volume.

Supplementary References

S1. Thomas, K. J.; Sheeba, M.; Nampoori, V. P. N.; Vallabhan, C.P.G.; Radhakrishnan, P. Raman spectra of polymethyl methacrylate optical fibres excited by a 532 nm diode pumped solid state laser. *Opt. A: Pure Appl. Opt.* **2008**, *10*, 055303.

S2. Zhang, J. M.; Zhang, D. H.; Shen, D. Y. Orientation study of atactic poly(methyl methacrylate) thin film by SERS and RAIR spectra. *Macromolecules* **2002**, *35*, 5140. b) Zhang, J. M.; Shen, D.Y. Near-infrared SERS study of the adsorption of a-PMMA dip-coated onto silver mirror substrate. *Chi. Chem. Lett.* **2002**, *13*, 563.

S3. Canamares, M. V.; Chenal, C.; Birke, R. L.; Lombardi, J. R. DFT, SERS, and Single-Molecule SERS of Crystal Violet. *J. Phys. Chem. C* **2008**, *112,* 20295.

S4. Le Ru E. C.; Etchegoin, P. G. *Principles of Surface enhanced Raman Spectroscopy and related plasmonic effects*, Elsevier, Amsterdam, The Netherlands **2009**.

S5. Cho, W. J.; Kim, Y.; Kim, J. K. Ultrahigh-Density Array of Silver Nanoclusters for SERS Substrate with High Sensitivity and Excellent Reproducibility *ACS Nano* **2012**, *6*, 249.

S6. Cai, W.; Ren, B.; Li, X.; She, C.; Liu, F.; Cai, X. Investigation Of Surface-Enhanced Raman Scattering From Platinum Electrodes Using A Confocal Raman Microscope: Dependence Of Surface Roughening Pretreatment. *Surface Science* **1998**, *406*, 9–22.